Wetting and Capillary Condensation as Means of Protein Organization in Membranes

Tamir Gil, Mads C. Sabra, John Hjort Ipsen, and Ole G. Mouritsen

Department of Chemistry, Technical University of Denmark, DK-2800 Lyngby, Denmark

ABSTRACT Wetting and capillary condensation are thermodynamic phenomena in which the special affinity of interfaces to a thermodynamic phase, relative to the stable bulk phase, leads to the stabilization of a wetting phase at the interfaces. Wetting and capillary condensation are here proposed as mechanisms that in membranes may serve to induce special lipid phases in between integral membrane proteins leading to long-range lipid-mediated joining forces acting between the proteins and hence providing a means of protein organization. The consequences of wetting in terms of protein aggregation and protein clustering are derived both within a simple phenomenological theory as well as within a concrete calculation on a microscopic model of lipid-protein interactions that accounts for the lipid bilayer phase equilibria and direct lipid-protein interactions governed by hydrophobic matching between the lipid bilayer hydrophobic thickness and the length of the hydrophobic membrane domain. The theoretical results are expected to be relevant for optimizing the experimental conditions required for forming protein aggregates and regular protein arrays in membranes.

INTRODUCTION

The study of the organization of integral proteins in membranes is important because the organizational state in many cases controls the functional state of the membrane system (Gennis, 1989; Kinnunen and Mouritsen, 1994). Furthermore, regular organization in terms of crystallization of membrane proteins within the membrane is of importance for making progress in determination of membrane protein structure (Kühlbrandt, 1992). The organizational state of integral proteins dispersed in lipid membranes is determined by a number of different physical forces and effects (Jackson, 1993; Watts, 1993). In addition to specific short-range protein-protein interactions and direct protein-lipid interactions, a host of indirect lipid-mediated protein-protein interactions and lipid-controlled effects are operative in controlling the nature of the organizational state of the lipid-protein assembly (Mouritsen and Bloom, 1993; Bruinsma et al., 1994; Fattal and Ben-Shaul, 1993; Aranda-Espinoza et al., 1996; Golestanian et al., 1996). Whereas the specific forces usually are of enthalpic origin, many of the indirect forces have a substantial component of entropy that acts in addition to the omnipresent entropy of mixing. A fundamental phenomenon in this connection is the underlying lipid bilayer phase equilibria and the way these equilibria are altered by interaction with the proteins (Mouritsen and Sperotto, 1992) as well as with extra-membrane components of the biological membrane, such as the cytoskeleton (Sackmann, 1994).

The main gel-fluid phase transition in pure lipid bilayers (Mouritsen and Jørgensen, 1994), with which we shall be concerned here, and its associated phase equilibria in mixed lipid bilayers imply different lipid phases and provide a cooperative mechanism for structuring and organizing the lipid bilayer assembly. Specifically, integral proteins may display different affinities for the various lipid phases and hence induce phase separation at appropriate thermodynamic conditions. Wetting is a particular thermodynamic phenomenon that depends on the lipid phase equilibria and is controlled by the conditions of the interface between the protein and the lipid matrix. In essence, the protein will at its surface stabilize the lipid phase to which it displays preferential affinity. This will in general lead to a local enrichment of that lipid phase at the interface. Under near-wetting conditions, the enrichment will extend over long ranges and eventually establish a thermodynamic phase at the wetting transition (Dietrich, 1988; Schick, 1990; Gil and Mikheev, 1995). For an assembly of proteins in a lipid bilayer, the wetting phenomenon can manifest itself as a capillary condensation of a special lipid phase (the wetting phase) in between the proteins. The enthalpic advantage in sharing the wetting phase among two or more proteins leads to an effective attraction between the proteins. Such a mechanism was conjectured to cause reversible aggregation of colloidal particles, called flocculation (Beysens and Esteve, 1985). Hence, the wetting phenomenon can induce long-range lipid-mediated forces between proteins and therefore act as a means of protein organization (e.g., clustering, aggregation, and crystallization) in lipid membranes.

In the present paper we shall investigate protein-induced wetting in lipid bilayers and propose wetting and capillary condensation as thermodynamic mechanisms for the organization of proteins in membranes. We shall point out that the lipid phase equilibria provide the necessary physical basis for wetting and that the specific thermodynamic conditions required for wetting and wetting-like phenomena to take place for a particular lipid-protein mixture can be

fulfilled by appropriate choices of temperature, chemical potential, and composition.

The paper presents a two-pronged theoretical approach to the problem in a two-dimensional geometry and is organized as follows. As a preamble and for the sake of completeness as well as to introduce wetting to the biophysics community, we describe the wetting concept for single circular objects (proteins) and the capillary force that acts between two wet objects. We then turn to the general phenomenology of wetting and capillary condensation for an assembly of circular objects (proteins). The problem is first discussed in terms of a simple ideal gas picture involving a phenomenological capillary potential that is analyzed to yield a cluster size distribution function. The analysis predicts a transition (phase separation), as a function of the chemical potential, from an exponential distribution, favoring small clusters, to a distribution with a peak corresponding to one large cluster (aggregate). Second, we study the phase equilibria of a binary lipid mixture with integral model proteins via a concrete calculation on a specific microscopic statistical mechanical model of lipid-protein interactions in membranes. This model takes for simplicity the hydrophobic matching (Mouritsen and Bloom, 1984, 1993) between the lipid bilayer thickness and the hydrophobic length of the protein as the main component of the direct, enthalpic lipid-protein interactions. The properties of the model, specifically the mode of protein organization, are derived using computer simulation techniques that faithfully and accurately account for the different contributions to the entropy. The generic predictions from the phenomenological model are compared with the results of the computer simulation calculations on the microscopic model. As neither of these theoretical approaches allow for a description of the formation of solid (crystalline) protein structures but only aggregates, the question of fluid–solid transitions within a patch of aggregated proteins is discussed separately in an Appendix. This question is of a fundamental nature and is linked to the still unresolved problem of crystallization and melting in two-dimensional systems (Bladon and Frenkel, 1995; and references within; Nielsen et al., 1996).

INTRODUCTION TO WETTING AND CAPILLARY CONDENSATION: THE CASES OF ONE AND TWO DISKS

To understand the phenomenology associated with the wetting of a circular object (disk) immersed in a two-dimensional fluid, we take the steps of introducing wetting in general, pointing out the differences between the cases of flat and round substrates, and between three and two spatial dimensions of the embedding system.

In general, when two thermodynamic phases, α and β, are close to coexistence, i.e., close to a first-order phase transition line, the presence of a substrate strongly preferring one of the phases leads to singular wetting effects (Dietrich, 1988; Schick, 1990). The preferred phase, β, tends to form

a layer intruding between the substrate and the other phase, α, even when the latter is stable in the bulk. In the complete wetting regime, the thickness, l_W, of the layer diverges continuously, $l_W \to \infty$, as the bulk $\alpha \to \beta$ phase transition line is approached. This continuous line of surface critical points may terminate at a wetting transition point, which can be first-order or critical (Fig. 1). A scaling description of the continuous wetting transition is achieved in terms of two orthogonal fields: one, chemical potential-like field, $\Delta\mu$, which measures the difference in the grand canonical potentials per unit volume of the two bulk phases; the other, temperature-like field, t, which is a generalized coordinate measuring the distance from the wetting transition point (μ_W, T_W) along the coexistence line shown in Fig. 1. In terms of these fields, the continuous growth of the wetting layer is characterized by the power laws $l_W \propto \Delta\mu^{-\Psi^c}$, $\Delta\mu \to 0^+$, in the complete wetting regime, and $l_W \propto t^{-\Psi}$, $t \to 0^+$, along the coexistence line. The values of the exponents Ψ^c and Ψ depend on the spatial dimension of the system under consideration (Dietrich, 1988; Schick, 1990).

Wetting of a planar (linear in the two-dimensional geometry) substrate has been extensively studied (Dietrich, 1988; Schick, 1990). When the underlying geometry of the $\alpha–\beta$ interface is planar (linear), uniform changes in the thickness of the wetting layer do not change the area (length) of the interface. Correspondingly, at the coexistence of the two bulk phases, $\Delta\mu = 0$, the equilibrium state of the wetting layer is determined by an interplay of the interfacial potential V and the thermal fluctuations. In particular, when the underlying geometry is planar (linear), nothing prevents the thickness from diverging when the effective interface-substrate interaction, resulting from renormalization of V by thermal fluctuations, is repulsive. However, increasing the
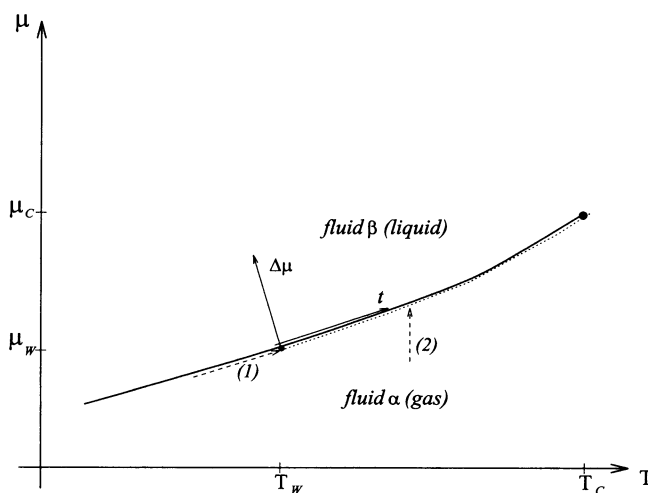

FIGURE 1   The generic phase diagram for wetting by one of two fluid phases (β) at the bulk coexistence line with the other (α), shown by a thick solid line. Critical wetting transition occurs at T_W by increasing the temperature along the $\alpha–\beta$ coexistence curve, as shown by path 1. For $T > T_W$, any path taken in the direction of the arrow (2) would terminate in a continuous complete wetting as the $\alpha–\beta$ coexistence curve is approached.

thickness of a wetting layer around a spherical or a cylindrical (circular), substrate leads to an increase in the area (length) of the interface. The corresponding increase in the interfacial free energy suppresses complete wetting at $\Delta\mu = 0$. Hence, the divergence of the mean thickness of the wetting layer can occur only in the limit where the curvature of the substrate vanishes, adding this curvature as a third field in the scaling description (Gil and Mikheev, 1995).

There is a crucial difference between wetting phenomena in two and three spatial dimensions that is due to the renormalizing effect of the capillary-wave fluctuations of the β-α interface between the wetting phase and the thermodynamically stable phase in the background. Because three is the marginal dimension for this renormalizing effect (Dietrich, 1998; Schick, 1990), the relative importance of these fluctuations for the thermodynamics of wetting phenomena in three dimensions is expected to be small compared with the direct forces involved, e.g., van der Waals forces. In two dimensions, however, (i.e., one-dimensional interfaces), the capillary-wave fluctuations play a dominant role, giving rise to an effective long-range repulsive force between the substrate and the fluid–fluid (α-β) interface, and exclude the possibility of prewetting transitions (Dietrich, 1998; Schick, 1990; Lipowsky and Fisher, 1987). As a result, once the direct substrate-interface interactions are not strong enough (above the wetting temperature, in the complete wetting regime) to hold the interface close enough to the surface of the substrate, the mean thickness of the wetting layer is determined by the balance between a disjoining pressure, which is induced by the capillary fluctuations and which tends to enlarge the mean thickness, and external pressures that tend to diminish it, e.g., hydrostatic pressure or gravity. Such a phenomenological picture was recently shown to apply in two dimensions to the wetting of a large circular substrate (disk) if a Laplace pressure is added to the pressure balance in the wetting layer (Gil and Mikheev, 1995).

The mean thickness of a two-dimensional wetting layer (one-dimensional interface) around a disk grows like $r_0^{1/3}$, for $r_0 \to \infty$, where r_0 is its radius, provided that $\Delta\mu \to 0^+$ and $T > T_W$ (Gil and Mikheev, 1995). Hence, a macroscopic wetting layer of thickness much larger than the molecular distances emerges at large values of r_0, validating the use of interface models in which the density profile of the fluid–fluid (α-β) interface is replaced by a sharp kink to which a local interfacial stiffness is attached (Dietrich, 1998; Schick, 1990). The stiffness of the α-β interface, denoted σ, defines a length scale in the system that we shall call the bulk correlation length,

$$\xi_b \equiv k_B T/\sigma, \qquad (1)$$

where k_B is the Boltzmann constant and T is the temperature. (Close to the bulk α-β critical point, T_C, where the bulk correlation length is assumed to be the same in the α and in the β phases, this definition coincides with the hyperscaling relation $\xi_b^{d-1} = \text{const} \cdot k_B T/\sigma$. However, the

theory here is relevant also for temperatures much lower than T_C). The *complete wetting regime* for the wetting of a disk is then defined by (Gil and Ipsen, 1997)

$$r_0 \gg \xi_b, \quad T_W < T < T_C \quad \text{and} \quad \sigma/r_0 \gg \Delta\mu \to 0, \qquad (2)$$

where T_C is the bulk α-β critical point and T_W is the wetting temperature for the analogous flat system. In this regime, the wetting of a disk is properly described by the effective interface grand canonical potential, parameterized by l, the mean thickness of the wetting layer,

$$\Omega(l) = 2\pi V(l) + 2\pi\sigma(r_0 + l) + \pi\Delta\mu[(r_0 + l)^2 - r_0^2], \qquad (3)$$

where $V(l) \equiv 0.948 \times r_0(k_B T)^2/(\sigma l^2)$ (Gil and Mikheev, 1995; Gil and Ipsen, 1997). The term $\pi\Delta\mu[(r_0 + l)^2 - r_0^2]$ in this equation accounts for the excess energy of the thermodynamically unfavorable β-phase, which covers an area of $\pi[(r_0 + l)^2 - r_0^2]$, $2\pi\sigma(r_0 + l)$ is the self-energy of the interface, and the first term represents the loss of configurational entropy involved in preventing the interface from crossing the surface of the substrate (Gil and Mikheev, 1995). $V(l)$ is of longer range than the relevant van der Waals substrate-interface interaction potential, which is proportional to r_0/l^{p-3} in the limit of $l \ll r_0$, where $p = 6$, 7 for nonretarded and retarded interactions, respectively (Gil and Mikheev, 1995), and is therefore the only relevant interaction potential in the problem (Lipowsky and Fisher, 1987). The case of wetting of a single disk is illustrated in Fig. 2, *a* and *b*, via microconfigurations generated in a computer simulation calculation on a microscopic interaction model to be described below.

Under the conditions that trigger wetting of a single disk, bringing two disks close to each other gives rise to two different topologies of the α-β interface line: one involving two separate loops, closing around each one of the disks individually (Fig. 3 (sep)), and one involving a single loop wrapping the two disks (Figs. 3 (bri) and 2 c). The latter is due to capillary condensation between the two disks that occurs to minimize the excess free energy that is associated with a given length of the α-β interface and a given coverage of the thermodynamically unfavorable β-phase. A transition between the separated and bridged configurations can be induced by tuning either the distance between the disks or by changing the thermodynamic conditions for the system, e.g., via $\Delta\mu$. Capillary condensation between two wet disks occurs already when the distance between the disks is of the order of their radius, r_0. It involves a dramatic increase in the local concentration (or rather the coverage) of the wetting phase β and introduces a new effective force in the system, giving rise to a net attraction between the disks (Gil and Ipsen, 1997). The aggregation force is caused by the tendency of the condensed system to reduce the length of the α-β interface and the coverage of the β-phase by reducing the distance between the disks. Very close to the phase transition, $\Delta\mu \to 0$, the attractive force between the aggregated disks is approximately constant and of size $F = 2(\sigma + \Delta\mu r_0)$ (Gil and Ipsen, 1997). For larger values
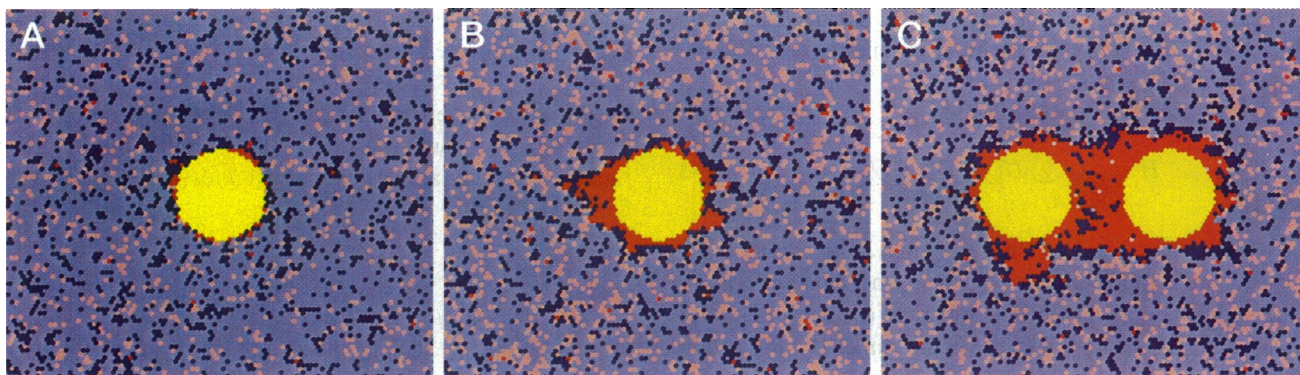
FIGURE 2   Illustration of wetting phenomena around circular disks embedded in a binary fluid near a $\alpha \rightarrow \beta$ phase transition (e.g., proteins embedded in binary lipid bilayers). The disks (the proteins), which have preference for phase β, are labeled by large yellow dots. The two species (the lipids) are labeled by red and blue small dots, respectively, and the two phases are indicated by dark (β) and light (α) colors, respectively. (a) The case of a single disk away from the wetting regime where only a microscopically thin layer of phase β is present at the interface corresponding to the case of interfacial adsorption. (b) The case of a single disk close to wetting. A thick layer of phase β is nucleated at the surface of the disk. (c) The case of two nearby disks close to wetting where the wetting layers overlap leading to capillary condensation. The data for the figures are obtained from computer simulation calculations on the microscopic model of lipid-protein interactions.

of $\Delta\mu$, F falls almost linearly with the distance between the disks. In the case of the conditions given in Eq. 2, the force can properly be derived from an effective interfacial free energy consisting of the same ingredients as in Eq. 3. This free energy is an analytical approximation that is based on a simple construction in which the differentiability of the interface configuration is relaxed in the small regions where the interface is detaching from the single disk to bridge between the two disks. Capillary-wave fluctuations were shown not to effect the mean location of the interface in the regions where it bridges between the two disks and that, to leading order, the location of the remaining interface is given by the theory for the single disk (Gil and Ipsen, 1997). The case of wetting of two adjacent disks leading to capillary condensation between the disks is illustrated in Fig. 2 c via a microconfiguration generated in a computer simulation calculation on a microscopic interaction model to be described below.
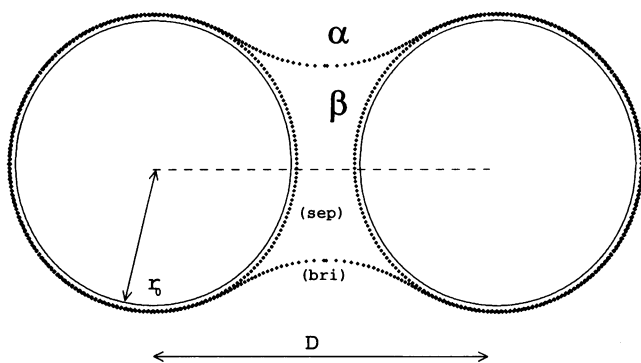

FIGURE 3   Two two-dimensional disks of radius r_0 separated at a distance D. The wetting layers surrounding each one of the disks (sep) remain separated until $\Delta\mu$ is sufficiently small to allow for the formation of a bridging interface (bri).

PHENOMENOLOGICAL MODEL OF WETTING IN LIPID-PROTEIN MEMBRANES: AGGREGATION OF MANY DISKS DUE TO CAPILLARY FORCES

We now consider a system of N identical β-preferring mobile disks of radius r_0, immersed in an α fluid. According to the study of capillary condensation between two disks (Gil and Ipsen, 1997), it is reasonable to expect that by tuning the chemical potential for the fluids close to the α–β transition line (but on the α side) one would reach a region where the disks tend to aggregate and form clusters of disks with a β-rich phase filling the space between them. When neglecting direct interactions between the disks (apart from the excluded-volume hard-disk interactions), the size of those clusters and the cluster-size distribution are controlled by the balance between different entropy effects and the capillary forces that are involved in minimizing the total length of the α–β interface and the coverage of the β-phase. The tendency to increase translational entropy would push the disks apart as well as give rise to a certain cluster-size distribution once clusters are formed. The way the disks (colloids) would arrange themselves inside the clusters is controlled by the interplay between configurational entropy, dominating in the colloid fluid phase, and the entropy of free volume per disk, dominating in the colloid crystalline phase (Hoover and Ree, 1968).

Ideal gas paradigm

To obtain an approximate cluster-size distribution function for a dilute collection of identical disks, we map the system of clusters of different sizes onto a mixture of noninteracting gas particles of different masses. The sizes (masses) of the clusters are parameterized by m, which denotes the number of disks in a cluster. By n_m we denote the number of clusters consisting of m disks and by $\{n_m\}$ a distribution

of cluster sizes. Given a set $\{n_m\}$ and ignoring the kinetic contribution, we can write the internal energy (the Hamiltonian) of such a system as

$$H = \sum_{m=1}^{\infty} \sum_{k=1}^{n_m} U_k = \sum_{m=1}^{\infty} n_m U_m, \tag{4}$$

where $\{n_m\}$ is subject to the restriction $\sum_{m=1}^{\infty} mn_m = N$, where N is the total number of disks in a given realization of the system. U_m is a phenomenological capillary potential that is yet to be defined and that is the same for all clusters of size m.

With the help of a chemical potential, ν, that controls the total number of disks in the system, we can define and calculate the grand partition function of the system as follows:

$$\Xi = \sum_{n_1=0}^{\infty} \sum_{n_2=0}^{\infty} \cdots \sum_{n_m=0}^{\infty} \cdots \frac{1}{n_1! \, n_2! \cdots n_m! \cdots}$$

$$\times \prod_i \int \frac{d^2 r^i}{s^2} \{\exp[(\nu N - H)/k_B T]\} \tag{5}$$

$$= \prod_{m=1}^{\infty} \sum_{n=0}^{\infty} \frac{1}{n!} \left[e^{(m\nu + k_B T \ln A - U_m)/k_B T} \right]^n$$

$$= \exp\left\{ \sum_{m=1}^{\infty} \exp[(m\nu + k_B T \ln A - U_m)/k_B T] \right\},$$

where $\prod_i \int d^2 r^i$ indicates a multiple integral over all possible positions, r_i, of every cluster in a given cluster-size distribution $\{n_m\}$. As H is r independent, each one of these integrals produces the dimensionless area parameter $A\Xi$ $\int d^2 r/s^2 = $ (area of the system)$/s^2$, where s is the mean molecular nearest-neighbor separation in the system under consideration. In Eq. 5 we have coupled ν to the total number of disks, $N = \sum_{m=1}^{\infty} mn_m$, for each distribution $\{n_m\}$, and integrated over all possible distributions and thus over all possible values of N. The corresponding grand potential $\mathcal{A}$ is readily given by

$$\mathcal{A} = -k_B T \sum_{m=1}^{\infty} \exp[(m\nu + k_B T \ln A - U_m)/k_B T]. \tag{6}$$

From the form of the Hamiltonian in Eq. 4 we see that the average number of clusters of size m', $\langle n_{m'} \rangle$, is the partial derivative $\partial/\partial U_{m'}$ of $\mathcal{A}$. In general, for any m, we get

$$\langle n_m \rangle = \exp[(m\nu + k_B T \ln A - U_m)/k_B T]. \tag{7}$$

Phenomenological capillary potential

Let us now assume that the clusters under consideration are surrounded by a well defined interface line of stiffness σ

that separates a region consisting only of the β-phase, with the disks immersed in it, from an α background phase. We denote by ρ the number density of the disks inside the cluster and ignore for simplicity its dependence on the size of the clusters. Such clusters will minimize the length of interface per unit area by having an underlying geometry of a circle of radius

$$R_m = \sqrt{\frac{m}{\pi \rho}}. \tag{8}$$

For large m, we can approximate the energy associated which each cluster by replacing r_0 in Eq. 3 with R_m and by neglecting the contribution to the free energy coming from the wetting layer that surrounds the whole cluster. Accordingly, we obtain an approximative phenomenological potential

$$U_m = 2\pi R_m \sigma + \pi \Delta\mu(R_m^2 - mr_0^2)$$

$$= 2\sqrt{\frac{\pi}{\rho}} \, \sigma \sqrt{m} + \Delta\mu\left(\frac{1}{\rho} - \pi r_0^2\right)m. \tag{9}$$

The first term in Eq. 9 is the self energy of a circular interface of radius R_m and stiffness σ. The second term couples the area that is covered by the thermodynamically unfavorable β-phase to the potential difference per unit area, $\Delta\mu$, between the β-phase and the thermodynamically favorable α-phase. Close to the α–β first-order phase transition line ($\Delta\mu = 0$), fluctuations of the α–β interface line against an effective substrate consisting of disks in high density will increase the total length of this interface and the total coverage of the β-phase. As it will turn out, however, this will have only a marginal effect on the cluster-size distributions resulting from the simplified considerations we have introduced above.

Cluster-size distribution

With U_m at hand (Eq. 9) we can rewrite the cluster-size distribution function of Eq. 7 as

$$\langle n_m \rangle = Ae^{-(a\sqrt{m} + b \cdot m)/k_B T}, \tag{10}$$

where

$$a \equiv 2\sqrt{\frac{\pi}{\rho}} \, \sigma \tag{11}$$

and

$$b \equiv \Delta\mu\left(\frac{1}{\rho} - \pi r_0^2\right) - \nu. \tag{12}$$

We immediately notice that if b turns negative, n_m diverges with m, causing the divergence of the capillary potential $\mathcal{A}$ in Eq. 6. This indicates a phase transition from a phase that consists of finite (small) clusters of disks, of which the size distribution is given by Eq. 10, to a phase that is rich in disks and the β-fluid. In a system of a fixed disk concen-

tration, this would correspond to a phase separation in which all the disks would aggregate into a single cluster. In such a system the chemical potential ν would depend on the number of disks. In the thermodynamic limit, we can get an idea of this dependence by relating an $\langle N \rangle$-dependent potential, $\Omega(\langle N \rangle)$, to $\mathcal{A}$ in the standard way:

$$\mathcal{A} = \lim_{A \to \infty} [\Omega(\langle N \rangle) - \nu \langle N \rangle], \tag{13}$$

where

$$\langle N \rangle = \sum_{m=1}^{\infty} m \langle n_m \rangle = \sum_{m=1}^{\infty} m \times A e^{-(a\sqrt{m} + b \cdot m)/k_B T} \tag{14}$$

is the expectation value of the total number of disks in the system. The conditions at the phase separation are those at which the free energy of the system that consists of many (small) clusters is equal to the free energy of the system consisting of a single (large) cluster. An estimate for the former is given by $\Omega(\langle N \rangle)$ in Eq. 13, but a proper description of the latter is not challenged by this paper. However, the largest expectation value of the disk density, $\langle N \rangle/A$, in a system with an exponentially decaying cluster-size distribution can easily be obtained by setting $b = 0$ in Eq. 14. Upon replacing the sum by an integral, this yields

$$\frac{\langle N \rangle}{A} = 2e^{-a/k_B T}$$
$$\times \left[\left(\frac{k_B T}{a} \right) + 3 \left(\frac{k_B T}{a} \right)^2 + 6 \left(\frac{k_B T}{a} \right)^3 + 6 \left(\frac{k_B T}{a} \right)^4 \right]. \tag{15}$$

Without excluding the possibility that phase separation may occur at lower values of $\langle N \rangle/A$, Eq. 15 provides the upper limit, above which the system certainly undergoes a phase separation.

In the regime where the disks are distributed in many clusters of different sizes according to Eq. 10, we define a probability function, $p(m)$, of finding a disk within a cluster of size m by (cf. Eq. 14)

$$p(m) \equiv \frac{m \langle n_m \rangle}{\langle N \rangle} = A \frac{m}{\langle N \rangle} e^{-(a\sqrt{m} + b \cdot m)/k_B T}. \tag{16}$$

$p(m)$ is the fraction of disks found in clusters of size m out of the total number of disks, $\langle N \rangle$, and it exhibits a maximum at $m^* = (\sqrt{a^2 + 16b k_B T} - a)^2/16b^2$ for a positive b. Equation 16 can be very useful when it comes to identifying points of interest in relation to specific cluster sizes. For example, it can be applied to identify the critical disk concentration, say δ_C, above which most of the disks are expected to be found within clusters rather than as monomers. For $\langle N \rangle/A = \delta_C$ the probability of finding a disk as a monomer, $p(1)$, is exactly ½, and Eq. 16 with $m = 1$ can be

applied to calculate the corresponding critical value of b,

$$b_C = k_B T \ln \frac{2A}{\langle N \rangle} - a. \tag{17}$$

Substituting b_C into Eq. 14 and solving for $\langle N \rangle/A$ will give us the desired value of δ_C.

It is important to notice that, in our formulation of the problem for a fixed number of disks, b is eliminated by solving Eq. 14. Thus, the dependence of the cluster-size distribution $\langle n_m \rangle$ on $\Delta \mu$ comes in through a, which is a function of the disk density inside the clusters, ρ. ρ and $\Delta \mu$ are proportional to each other for values of $\Delta \mu$ that are not too small (see Eq. 22 below). Hence, upon reducing $\Delta \mu$ we increase a, thereby changing $\langle n_m \rangle$ and approaching the phase separation (see Eqs. 10, 14, and 15).

Wetting transition in the single-aggregate regime

A key result of our phenomenological model of wetting and capillary condensation in lipid-protein membranes is that aggregation of many wet disks due to capillary forces gives rise to patterns that are dominated by either many finite (small) clusters or a single large one. The single large cluster, which absorbs all the proteins, is a result of a phase separation in systems where the number of proteins is kept constant. Two interesting questions are related to the existence of the large cluster. First, how is the lateral arrangement of the disks inside the cluster, and second, how does the size of this cluster grow when the wetting transition ($\Delta \mu \to 0$) is approached? It is clear that the simplified internal energy of Eq. 9 cannot be the basis for a complete answer to these questions. A qualitative impression of how the arrangements of disks can be varied upon decreasing $\Delta \mu$ can be obtained from the microconfigurations to be described in Fig. 4, b–e below. A detailed and rigorous study of these problems is beyond the scope of this paper, and in this subsection we shall restrict ourselves only to the regime where the number density, ρ, of the disks inside the aggregate is small enough to allow us to treat them as ideal gas particles. In the Appendix we outline the key lines of a study of the formation of regular protein arrays (crystalline solids) within a large protein aggregate.

The regime of small ρ can be reached only if $\Delta \mu$ and σ are small enough, reducing the energy cost of filling the space among the N disks by the β-phase. Then one can think of a wetting transition in the sense of the divergence of the coverage of the β-phase, i.e., the divergence of $R_N = \sqrt{N/(\pi \rho)}$. Such a divergence necessarily involves singularities in $\Delta \mu$, σ, or N. In the region of these singularities, we can obtain the leading behavior of R_N by writing down the pressure balance within the aggregate (Gil and Mikheev, 1995):

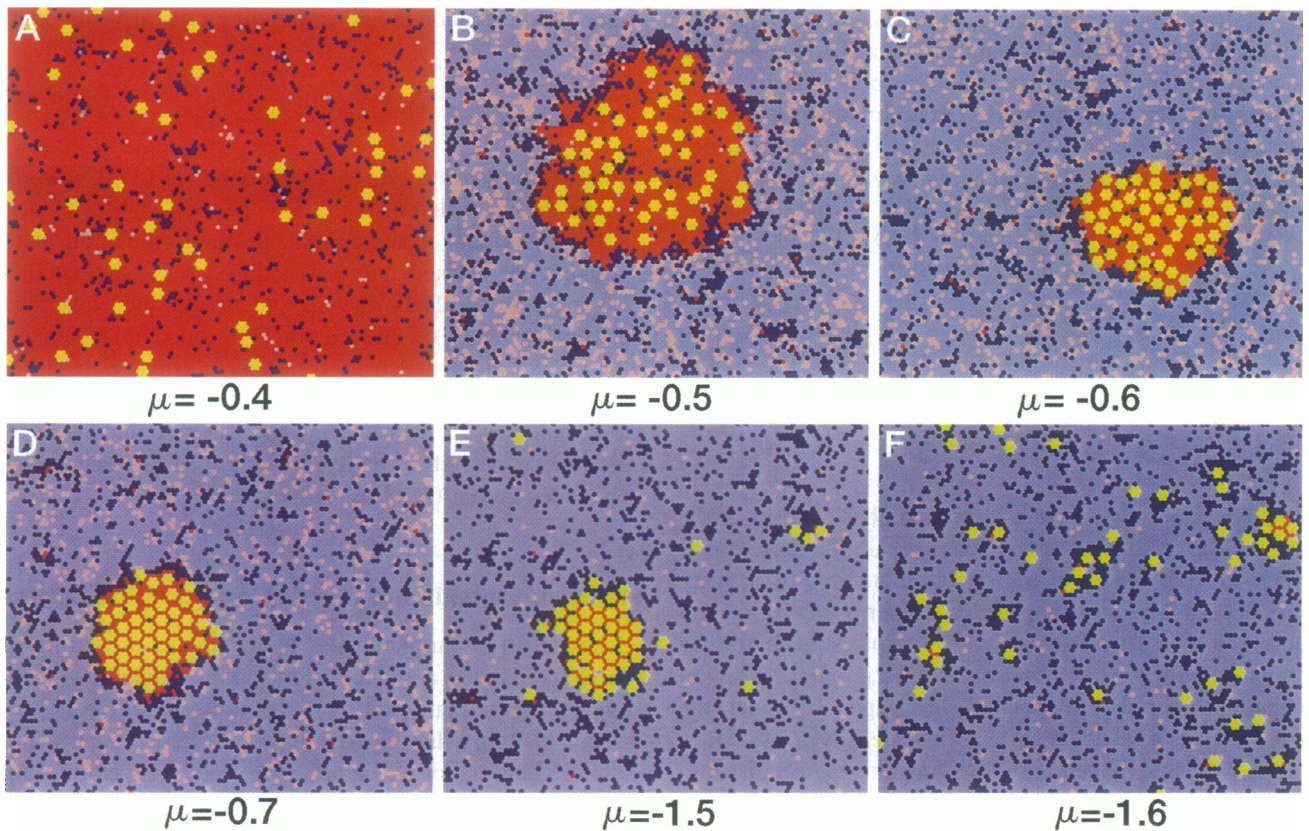$$\Delta \mu + \sigma/R_N = Z \rho k_B T = Z \frac{k_B T N}{\pi R_N^2}, \tag{18}$$

FIGURE 4   Microconfigurations of a binary lipid mixture with a dispersion of integral membrane proteins representative of a series of different values of the chemical potential, μ, which controls the lipid composition in a broad region around a phase separation between two lipid phases, α (gel) and β (fluid). The data are obtained from computer simulation calculations on the microscopic model of lipid-protein interactions. The proteins, which have preference for phase β (dark red), are labeled by large yellow dots. The two lipid species are labeled by red and blue small dots, respectively, and the two phases are indicated by dark (β) and light (α) colors, respectively. The configurations (a–f) are each labeled by the corresponding value of the chemical potential, μ, in units of 10^{-13}erg. The temperature is $T = 307$ K, and the parameters used for the modeling correspond to the case of a mixture of DMPC and DSPC and a model protein of hydrophobic length of $d_P = 42.5$ Å. Each model protein covers an area corresponding to $n_P = 7$ lipid acyl chains, similar to bacteriorhodopsin. The system comprises 100×100 acyl chain sites.

where $Z \equiv P/(\rho k_B T)$ is the compressibility factor and P is the pressure resulting from the colloid hard disk interactions within the aggregate. Here we have equated this expansion pressure with the shrinking pressure due to the chemical potential difference and the Laplace pressure. Z can be written as the virial expansion for the equation of the state of the hard disks,

$$Z = 1 + B_2\rho + B_3\rho^2 + B_4\rho^3 + \ldots, \qquad (19)$$

where B_n are the virial coefficients.

In the limit where $R_N \to \infty$ and $\rho \to 0$, Z in Eq. 19 becomes 1, i.e.,

$$\Delta\mu + \sigma/R_N = \frac{k_B T N}{\pi R_N^2}. \qquad (20)$$

Here we already notice that for a finite N, a wetting transition, $\Delta\mu \to 0$, can only occur if $\sigma \to 0$, e.g., when $T \to T_C$, T_C being the α–β bulk critical point. However, even for $T < T_C$, R_N can diverge if $N \to \infty$. According to Eq. 20, the asymptotic regime can be divided into two: $\Delta\mu \gg \sigma/R_N$ and $\Delta\mu \ll \sigma/R_N$. The first regime can certainly be reached

for any finite $\Delta\mu > 0$ by increasing N and therefore increasing R_N, and the second one is certainly relevant when $\Delta\mu = 0$. These observations are summarized in the following relations

$$R_N \approx \begin{cases} \sqrt{k_B T N/(\pi\Delta\mu)} \sim N^{1/2}, & \sigma^2/\Delta\mu \ll k_B T N \\ k_B T N/(\pi\sigma) \sim N, & \sigma^2/\Delta\mu \gg k_B T N, \end{cases} \qquad (21)$$

where we have assumed that σ does not change significantly when $\Delta\mu \to 0$. Eq. 21 predicts that for a small enough $\Delta\mu$, R_N can cross from a region of linear growth with N to a power-law growth behavior with the power ½. Corrections to the leading behavior must involve terms of higher order in ρ in Eq. 19 and are beyond the scope of this paper. The dependence of ρ on N within the asymptotic region of Eq. 21 can be calculated from it to give

$$\rho(N) \approx \begin{cases} \Delta\mu/k_B T \sim \text{const.}, & \sigma^2/\Delta\mu \ll k_B T N \\ \pi\sigma^2/[N(k_B T)^2] \sim 1/N, & \sigma^2/\Delta\mu \gg k_B T N, \end{cases} \qquad (22)$$

from which we see that in the case where $\Delta\mu$ is not too close to zero, ρ is independent of the number of disks inside the aggregate. We shall return to this point in the section where

we compare the results from this phenomenological approach with the results from the microscopic modeling.

MICROSCOPIC MODEL OF WETTING AND PROTEIN-INDUCED PHASE EQUILIBRIA IN MEMBRANES

In this section we introduce a simple statistical mechanical model of lipid-protein interactions in lipid bilayers with just enough complexity to allow, via Monte Carlo computer simulation techniques, for calculation of the phase equilibria and the changes on these equilibria due to the presence of an annealed dispersion of model proteins. Theoretical biophysical studies of lipid-protein interactions is a matter of making a proper balance between details and degree of realism on the one hand and computational feasibility on the other hand. Accurate and elaborate molecular force fields together with fast molecular dynamics simulation algorithms (Damodaran and Merz, 1994) have led to substantial advances in our understanding of molecular details of lipid-protein interactions. However, due to the complexity of this type of approach, modern computers permit only a rather small number of molecules (in most cases only a single protein dissolved in some hundred lipid molecules) to be studied, which at the moment excludes studies of phase equilibria, protein aggregation phenomena, and strongly fluctuating interfacial phenomena like wetting. We are therefore forced to study simpler statistical mechanical lattice models with phenomenological potentials (Mouritsen et al., 1996) and to investigate them by stochastic (Monte Carlo) computer simulation methods (Mouritsen, 1990). Using a simple model is both the shortcoming and the strength of the present approach. Obviously, a simple model leaves out a number of molecular details that can be important. The strength is that it can handle cooperative phenomena in a transparent fashion and it allows for a study of strongly fluctuating phenomena near phase transitions, which is a striking characteristic of lipid-bilayer behavior. Moreover, the influence of various parameters, such as temperature, chemical potential and composition, and type of lipid species as well as size of protein can readily be investigated.

As both details of the microscopic model as well as the numerical simulation method have been described in detail elsewhere (Mouritsen et al., 1996; Dammann et al., 1996) we shall restrict ourselves to a very brief description and then focus on the results obtained.

Model

The model is a microscopic version of the mattress model of lipid-protein interactions in membranes (Mouritsen and Bloom, 1984), which focuses attention on one particular aspect the interaction, being the hydrophobic matching of lipid bilayer thickness, d_L, and hydrophobic length, d_P, of the protein. Again, this is a restriction in realism of the

modeling, but it provides the advantage of being able to isolate the effects due to a purely physical and nonspecific interaction. The hydrophobic mismatch interaction is anticipated to be important when it comes to a determination of phase equilibria involving the main gel-fluid phase transition because the bilayer thickness changes typically 10–20% in the transition region. To further focus on the effects of mismatch we shall here be concerned with binary mixtures of lipids with the same zwitterionic headgroups (phosphatidylcholine, PC) but with different acyl chain lengths, specifically dimyristoylphosphatidylcholine (DMPC) and distearoylphosphatidylcholine (DSPC).

The model we use for the binary lipid mixture in a pseudo-two-dimensional planar phase is a special version of a 10-state lattice-gas model (Pink et al., 1980) developed to describe the phase equilibria in mixtures of lipids with different acyl chain lengths (Risbo et al., 1995; Jørgensen and Mouritsen, 1995). The 10 internal states and the associated degeneracies of each lipid species reflect the internal conformational statistics of long hydrocarbon chains. The model faithfully describes the phase equilibria of highly nonideal mixtures such as DMPC-DSPC. In particular it describes the broad gel-fluid phase coexistence region (Jørgensen and Mouritsen, 1995) in which the gel phase predominantly consists of the long-chain lipid DSPC, which has the higher transition temperature, and in which the fluid phase is mainly made up by the short-chain lipid DMPC. The interaction with integral membrane proteins is taken into account by parameterizing the lipid-protein interaction in terms of the mismatch, $|d_L - d_P|$ (Mouritsen et al., 1996).

The Hamiltonian of the model can formally be written as

$$\mathcal{H} = \mathcal{H}_0 - \sum_{\langle i,j \rangle} \sum_{p,q} (J_{pq} \mathcal{L}_i^p \mathcal{L}_j^q + K_p^P \mathcal{L}_i^p \mathcal{P}_j) - \mu \sum_i (\mathcal{L}_i^p - \mathcal{L}_i^q)$$

$$+ J_{PP} \sum_{\langle i,j \rangle} \mathcal{P}_i \mathcal{P}_j, \qquad (23)$$

where $\mathcal{L}_i^p = 0, 1$ is the site occupation variable for the two lipid species, p, $q = 1, 2$, and $\mathcal{P}_j = 0, 1$ is the site occupation variable for the protein. $\mathcal{H}_0$ is a single-site energy including the acyl chain intramolecular conformational energy and an interfacial pressure-area term (Pink et al., 1980). J_{pq}, J_{PP}, and $K_p^P = K|d_L^p - d_P|$ are interaction constants. J_{pq} depends on the conformational state of the two involved acyl chains, and $\mathcal{L}_i^p$ has an implicit dependence on the acyl chain conformational state. Details regarding the values of the various interaction constants can be found in Mouritsen et al. (1996). The interactions are restricted to nearest neighbors on a triangular lattice. The lipid composition, $x_p = (2C)^{-1} \sum_i \mathcal{L}_i^p$ and $x_q = (2C)^{-1} \sum_i \mathcal{L}_i^q$, with $C = \frac{1}{2}(\mathcal{N} - \sum_j \mathcal{P}_j + n_p^{-1} \sum_j \mathcal{P}_j$, is controlled by the chemical potential μ, where $\mathcal{N}$ is the number of sites on the lattice, each of which is either occupied by a lipid acyl chain (i.e., one-half of a lipid molecule) or a fraction, n_P^{-1}, of a protein. Each protein is taken to occupy n_P lattice sites arranged in a compact hexagonal shape. The protein concentration, $x_P = 1 - x_p - x_q = (n_P C)^{-1} \sum_j \mathcal{P}_j$, is fixed.

Computer simulation techniques

The stochastic dynamics of the model (Mouritsen, 1990) used to bring the mixture in equilibrium with a thermal bath, characterized by a temperature T, and with a lipid particle reservoir, characterized by a chemical potential μ, is Glauber dynamics for internal transitions within each lipid species, Glauber dynamics for exchange of lipid particles with the reservoir, and extended Kawasaki lipid-protein exchange corresponding to diffusional motion of the protein in steps of one lattice constant. The lipids that have to be displaced in front of a moving protein are translocated to the vacant sites behind the protein. The acceptance criterion is given by the standard Monte Carlo Metropolis rate, $\min\{1, \exp(-\Delta\mathcal{H}/k_B T)\}$. For simplicity, all pair exchanges are taken to occur on the same time scale (given in units of Monte Carlo steps per lattice site, MCS); i.e., the two species and the proteins are taken to have the same diffusion constant.

The Monte Carlo simulations are performed on finite triangular lattices with $\mathcal{N} = L \times L$ sites subject to periodic boundary conditions. Different lattice sizes have been considered and most of the results reported below refer to $L = 100$.

Results of the model simulations

The advantage of model simulations of the type described above is that they, in addition to standard thermodynamic functions and various correlation functions, can provide information on the lateral organization of the mixed system under different conditions. As our main interest here is the lateral organization of the many-particle system and in particular the phase behavior and how wetting phenomena may influence this behavior, we shall restrict ourselves to present a series of microconfigurations representative of these different conditions.

In Fig. 4 is shown a gallery of microconfigurations corresponding to a fixed temperature, a fixed protein concentration, and fixed model parameters. The only parameter being varied is the chemical potential, which controls the phase equilibria via changes of the lipid composition. The corresponding cut through the lipid binary phase diagram is indicated in Fig. 5. This diagram corresponds to the absence of proteins but can be used as a guide to interpret the phase state of the systems shown in Fig. 4 because of the low protein concentration. A calculation of the complete phase diagram for the ternary mixture would be extremely elaborate and has not been carried out. It should be noted that, due to the phase transition, the lipid composition varies highly nonlinearly with μ near the phase boundaries.

Going through Fig. 4, a–f, corresponds to decreasing the chemical potential, μ, in Eq. 23 and therefore to an increase in x_{DMPC} at the expense of x_{DSPC} (p = DMPC and q = DSPC). The configuration in Fig. 4 a corresponds to a gel phase predominantly made up of DSPC, and the proteins are
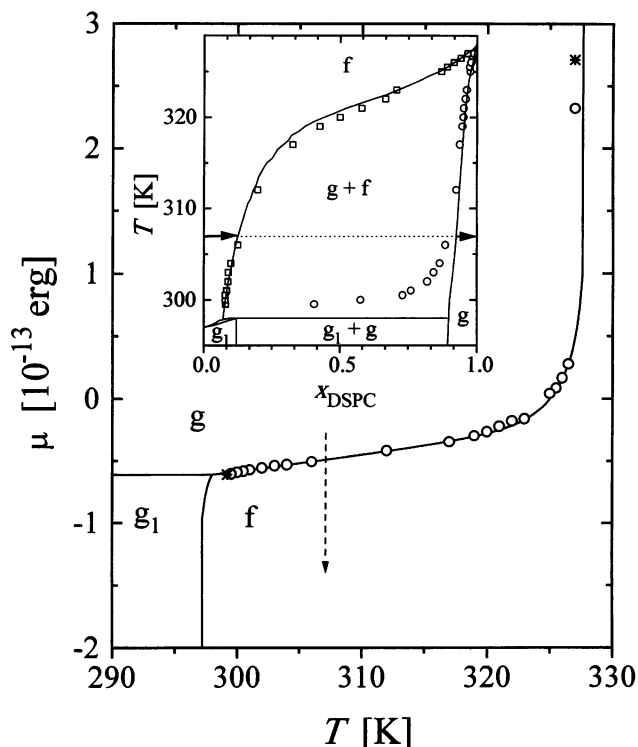

FIGURE 5   Schematic phase diagram for the DMPC-DSPC lipid mixture given in the $(T - \mu)$ plane with the dashed arrow indicating the chemical-potential path taken to obtain the series of microconfigurations in Fig. 4, a–f. The inset shows the corresponding phase diagram in the $(x_{DSPC} - T)$ plane with an indication of the same path. The points represent computer simulation data whereas the solid lines indicate the corresponding mean-field phase diagram (data from Risbo et al., 1995). It should be noted that there is a strongly nonlinear relation between chemical potential and composition, in particular close to the phase boundaries.

randomly distributed as there is no preferential coupling of the proteins to any of the available lipids.

In going from Fig. 4 a to Fig. 4 b we have just crossed the phase boundary to the gel-fluid coexistence region (cf. Fig. 5). The proteins are predominantly surrounded by lipids in the gel phase, mostly DSPC gel lipids but also a small concentration of DMPC gel lipids. The compositional fluctuations (Jørgensen et al., 1993; Mouritsen and Jørgensen, 1994) in both the gel phase and in the fluid phase are clearly seen. These compositional fluctuations are stronger the closer the system is to equimolarity. The interface between the gel and fluid regions is seen to be wetted (enriched) by DMPC lipids in their gel state. Due to the hydrophobic matching, this wetting layer tends to lower the interfacial free energy. Very close to the phase boundary, the gel phase can be considered a phase that is induced and stabilized by capillary condensation around the proteins. The existence of an interface with a nonvanishing stiffness, closing around the protein-gel aggregate in Fig. 4 b and not letting it grow continuously to infinity when increasing μ, suggests that the transition from Fig. 4 b to Fig. 4 a is of first order. As the chemical potential is further decreased (cf. Fig. 4, c–e), the fluid phase grows at the expense of the gel, and the proteins

are forming one large aggregate of a decreasing diameter. At the same time the compositional fluctuations are suppressed, because the composition is moving away from the equimolar one. In Fig. 4 d and e, the extent of the gel phase is now so small, compared with the amount of proteins, that the proteins pack tightly in a seemingly crystalline patch. The regularity of this protein array may be an artifact of the underlying lattice, and the protein aggregate should therefore only be considered a densely packed solid phase with no specification of its possible crystal symmetries. However, the close-packed crystalline protein crystal in Fig. 4 e can also be seen as a result of the excluded volume interactions acting between the proteins in the confined volume of the cluster. Such interactions would also lead to formation of crystalline solids even in the absence of an underlying lattice (Alder and Wainwright, 1962).

In the case of Fig. 4 e there are just enough gel-state DSPC lipids to cover the surface of the proteins, and the maximal amount of proteins are sharing annular lipids. Upon a further decrease of the fraction of DSPC lipids (Fig. 4 f) there are not enough DSPC lipids around to keep the protein aggregate together, and the entropy of mixing shifts the balance toward a dispersion of small protein clusters in the fluid phase. At this stage we have left the gel-fluid coexistence region. The transition from the state of a single large protein aggregate to a dispersion of very small protein clusters, most of them containing only a single protein, is very sharp. As is observed from Fig. 4 f and e, the small protein clusters are covered with a layer of gel-state DMPC lipids that provide a better hydrophobic matching than the fluid-state lipids. The few clusters of proteins left are glued together with the few remaining gel-state DSPC lipids.

The effect of wetting and capillary condensation on the organization of proteins in membranes is most clearly seen by inspecting Fig. 4, e and f. In going from Fig. 4 f to Fig. 4 e we are extremely close to the phase boundary between the fluid phase and the gel-fluid coexistence region (cf. Fig. 5). The proteins are wetted by the gel phase lipids, and the wetting layers are starting to overlap, inducing a capillary condensate that is just about to form a connected gel patch that, upon further increase of μ, will develop into a thermodynamic gel phase. Slight variations in μ or other system parameters in this region will have a dramatic and highly nonlinear effect on protein organization.

From a thermodynamic point of view, the variations in the system aggregational state is most naturally studied and mapped out in the grand canonical ensemble for the lipids, which corresponds to variations of the chemical potential as in Fig. 4. Obviously, under experimental conditions, μ is not the natural parameter to vary. Instead, one may want to vary temperature and lipid and protein composition as well as the type of lipids or proteins studied. However, the same type of scenarios shown in Fig. 4 can be obtained by varying one or more of these other variables. This is illustrated in Fig. 6, which in different cases shows the effects of 1) changing the strength of the hydrophobic mismatch interaction between the lipid bilayer and the protein, 2) changing

the protein concentration, 3) changing the cross-sectional area of the proteins, and 4) changing the temperature.

Choosing a protein with a stronger hydrophobic mismatch interaction between the lipid bilayer and the protein, Fig. 6, a to Fig. 6, b, enhances the affinity of the proteins to the gel-state lipids. This increases the extent of the gel-state lipids in the system, allowing for the existence of the single protein aggregate at lower values of μ in comparison with Fig. 4 e.

Increasing the concentration of the proteins, Fig. 6, a to Fig. 6, c, reduces the loss in the entropy of mixing of the proteins due to the aggregation in a single cluster, allowing for the existence of the single protein aggregate at lower values of μ in comparison with Fig. 4 e.

Choosing a protein with a larger cross-sectional area, i.e., a larger circumference, Fig. 6, a to Fig. 6, b, increases the gain in the favorable gel-protein interface and reduces correspondingly the unfavorable fluid-gel (fluid-protein) interface per aggregating protein (Gil and Ipsen, 1997). Thus, it enhances aggregation in comparison with Fig. 4 f.

The effect of increasing the temperature, for constant chemical potential, is illustrated in Fig. 6, e–g. Going from Fig. 6, e to Fig. 6, f, the effect of temperature is to enhance protein aggregation/crystallization within the protein-wetted phase due to a progressive lipid chain melting of the long-chain species. A further increase in temperature, Fig. 6, e to f, has two complementary effects that lead to the transition from a single protein aggregate to a dispersion of small protein clusters. First, as it is observed in the phase diagram of Fig. 5, it moves the system deeper into the fluid region, as decreasing μ would do but at a different rate, reducing the extent of the gel-state lipids in the system. Second, it increases the loss of the entropy of mixing of the proteins due to the aggregation in a single aggregate, favoring a state with a dispersion of small protein clusters.

In the thermodynamic limit, the lipid fluid-gel transition in the background of Fig. 4 b to Fig. 4 a can be approached continuously by increasing the number of proteins very close to the boundary of the gel-fluid coexistence region. This wetting-like transition can be characterized by monitoring the growth in the extent of the DSPC-rich gel phase as a function of the number N of the proteins. This is illustrated in Fig. 7 for three different values of μ in terms of the mean value of the radius of the protein aggregate, R_N, shown as a function of N. As μ is increased toward its value at the lipid fluid-gel transition, the power law $R_N \sim N^{1/2}$ changes into a linear growth law, $R_N \sim N$. These power laws and the crossover, which are consistent with the predictions of the phenomenological theory (cf. Eq. 21), are discussed in the following section.

DISCUSSION OF THE THEORETICAL RESULTS

The two different theoretical approaches to wetting and capillary condensation presented above each have their advantages and drawbacks. Whereas the phenomenological
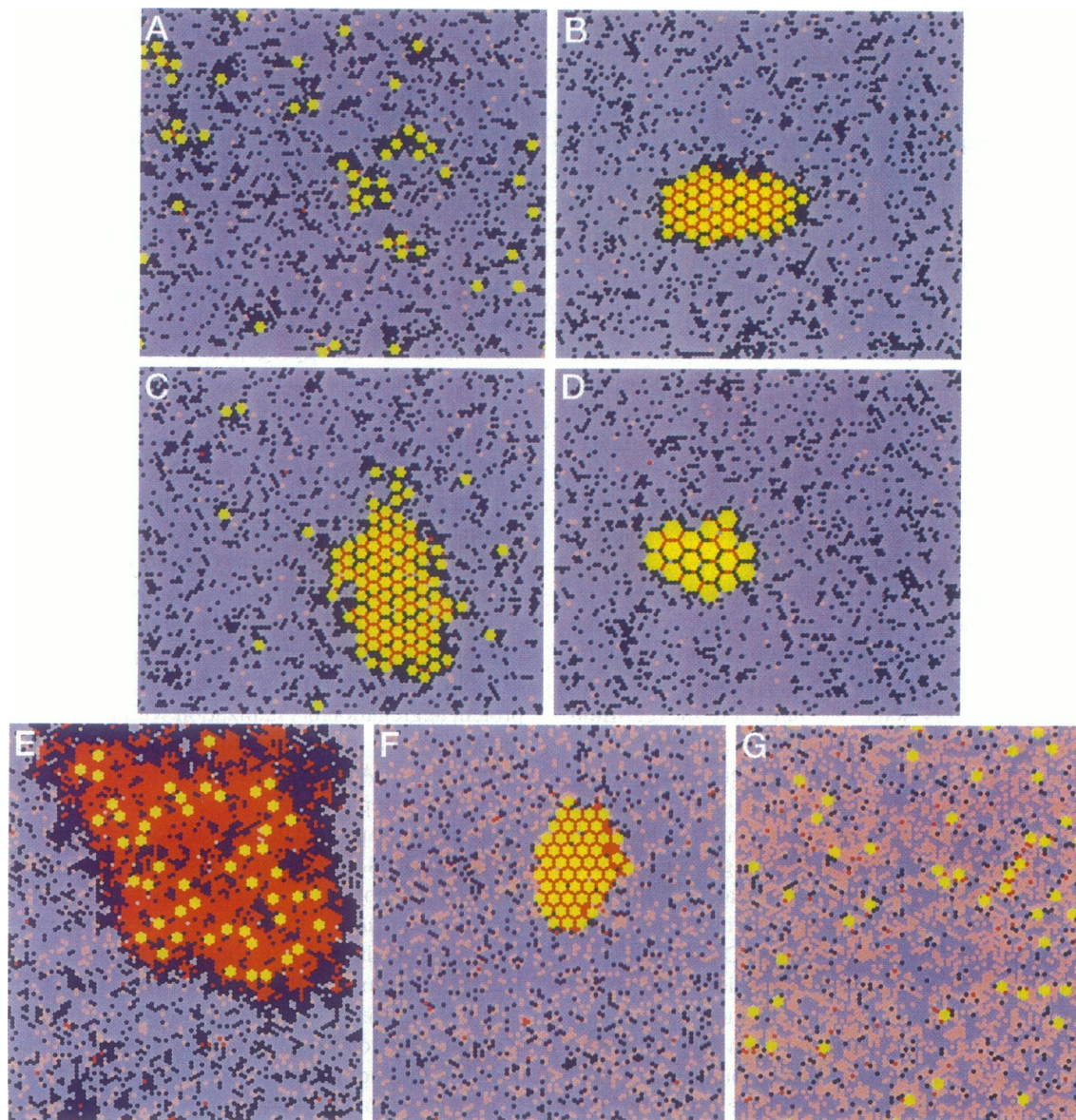
FIGURE 6 Microconfigurations of a binary (DMPC-DSPC) lipid mixture with a dispersion of integral membrane proteins. The different cases illustrate the effect of $(a) \rightarrow (b)$: changing the strength of the hydrophobic mismatch interaction between the lipid bilayer and the protein from $K = 0.5 \times 10^{-14}$erg to $K = 0.7 \times 10^{-14}$erg; $(a) \rightarrow (c)$: increasing the protein concentration from $x_P = 1/500$ to $x_P = 1/100$; $(a) \rightarrow (d)$: increasing the protein cross-sectional area from $n_P = 7$ to $n_P = 18$; and $(e) \rightarrow (f) \rightarrow (g)$: increasing the temperature from $T = 307$ K to $T = 325$ K to $T = 360$ K. The symbols and the color coding are as in Fig. 4.

theory involves approximations about the free energy and in particular about the various entropy contributions and yields no details about the microscopic states of the system, it provides the advantage of leading to an analytical expression for the capillary forces and the resulting cluster size distribution. The microscopic model and the associated simulations have their advantages in dealing with a microscopically based interaction potential, accounting accurately for the different entropy contributions and leading to details like microconfigurations, but they suffer from being a numerical approach, which is much less transparent in its general applicability and as to how the results depend on the various system parameters and thermodynamic potentials.

Together, the two approaches are, however, expected to constitute a fairly comprehensive approach to the problem of how wetting and capillary condensation may serve as means of protein organization in membranes.

With $\langle n_m \rangle$, b, and $p(m)$ at hand (cf. Eqs. 10, 14, and 16, respectively), the phenomenological theory puts us in a position to draw the qualitative picture that emerges from applying the ideal gas paradigm to estimate the cluster size distribution of aggregates of many wet disks. The asymptotic disk (protein) concentration determined by Eq. 15 can serve as a basis for comparison with the results obtained form the microscopic model simulations in the regions where phase separation occurs (cf. Figs. 4 and 6).
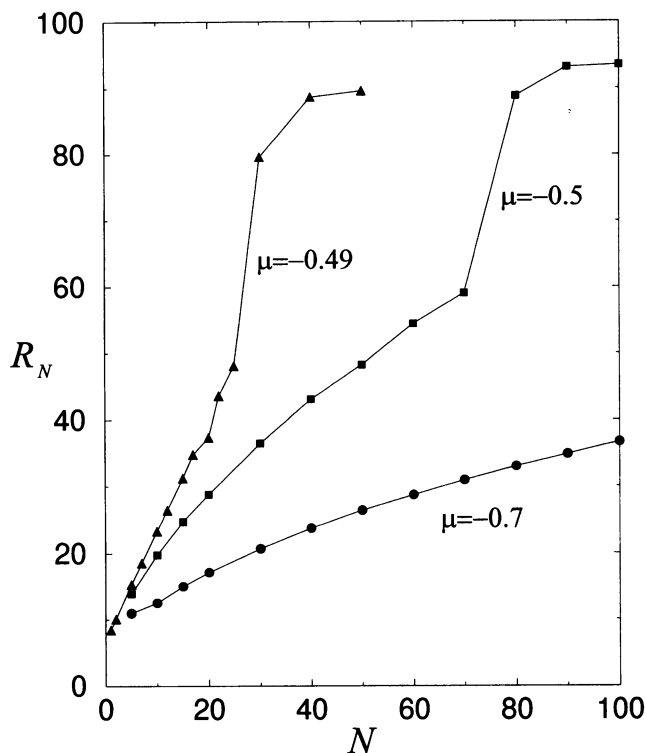
FIGURE 7 Mean radius, R_N, of the protein-gel (DSPC) aggregate separated from the DMPC lipid background. R_N is calculated from the mean coverage of the DSPC gel obtained by computer simulations in the region of the protein-induced phase separation for $\mu/(10^{-13} \text{erg}) = -0.7$ (●), -0.5 (■), and -0.49 (▲). The system comprises 100×100 acyl chain sites, and the lines connecting the data points are guides to the eye. The (discontinuous) jumps in the value of R_N at $N = 25$ and 65 for $\mu/(10^{-13} \text{erg}) = -0.49$ and -0.5, respectively, corresponds to a transition in which most of the lipid molecules become DSPC gel. The points of this transition cannot be approached continuously upon increasing N due to the small system size.

By decreasing the chemical potential μ (cf. Fig. 4, e and f) or the density of the disks in the system N/A (cf. Fig. 6, c and a) or by increasing the temperature T (cf. Fig. 6, f and g), we move the system through a transition from a state where the disks are aggregated in one large cluster to a state where the disks are distributed among smaller clusters. This corresponds to going through the conditions approximated by Eq. 15. Decreasing μ (Fig. 4) increases $\Delta\mu$ and the density ρ of the disks inside the clusters (cf. Eq. 22) and decreases thereby the value of $a \equiv 2\sigma\sqrt{\pi/\rho}$. This in turn increases the value of b in Eq. 14 and the limit value of the disk concentration in Eq. 15. The assumption that ρ is independent of the number m of disks that constitute a cluster is not too crude if clustering occurs when all the clusters are close-packed (cf. Fig. 4, e and f). Moreover, from Eq. 22 we learn that, for low values of $\Delta\mu$, ρ is proportional to $\Delta\mu$ and is m independent. When $\Delta\mu$ vanishes, ρ is inversely proportional to m, and the cluster size distribution $\langle n_m \rangle$ of Eq. 10 needs readjustment. These two regimes are observed in Fig. 7 where for a range of values of $\Delta\mu$, corresponding to Fig. 4, b–e, $R_N \sim \sqrt{N}$, indicating

a ρ that is m independent. As $\Delta\mu \to 0$, the behavior of R_N crosses over to a linear relation, $R_N \sim N$, indicating a ρ that is inversely proportional to m (cf. Eqs. 21 and 22). For intermediate values of $\Delta\mu$, where the disks lie close to each other but are not close-packed, excluded volume effects and the competition between configuration and free volume entropies (cf. Appendix) complicate the analytical representation of the compressibility factor in Eq. 19 beyond the scope of this paper.

The phenomenological model is primarily relevant to the limit of dilute systems where the configurational entropy for the mixture of ideal gases can be applied. Moreover, we have ignored the momentum impact on the free energy, which is relevant in the cases where aggregates can transfer momentum to each other by collisions, but one could incorporate this aspect relatively easy within the framework of the present study. Approximating all the clusters to be circular and of radius R_m (Eq. 8) has on the one hand favored small aggregates by relating to them smaller areas and perimeters than the actual ones. On the other hand, ignoring the outer wetting layers has lowered the potential of aggregates of size m by a term proportional to $m^{1/6}$ (Eq. 9), favoring the large aggregates. A cancellation of these two types of errors is plausible but is not addressed in the present study.

It should also be noted that the disks (proteins) considered in the simulations are rather small and the curvature of their surface lines prevents the development of a wetting layer. The disks are therefore not wet when immersed in the α-phase considered in the phenomenological theory. A further refinement would, therefore, at large values of $\Delta\mu$ involve two different values of the interfacial stiffness, σ, one for the interface surrounding the cluster and one for the interfaces of the disks inside the cluster. This will, however, not change the qualitative observations of Figs. 4, 6, and 7.

CONCLUSIONS

We have in the present paper studied wetting and capillary condensation phenomena as means of organizing proteins in lipid membranes. It was pointed out that the cooperativity of lipid bilayers contains the necessary physics to allow such phenomena to occur and that the specific conditions required can be fulfilled by appropriate choices of thermodynamic parameters. We have discussed the phenomena in the simplest possible setting with the advantage of being able to unravel the general structure of the problem and the obvious drawbacks of not being able to make quantitative comparisons with specific experimental systems. The simplicity and generality of our approach should, however, provide a guide for experimentalists to optimize the conditions for protein aggregation and protein crystallization in protein-lipid recombinants. Whereas the phenomenological model presented in this paper is fairly general and insensitive to details of the actual molecular potential acting in specific systems, the most severe shortcoming of our microscopic

model is its neglect of electrostatic forces, which are crucial for many lipid-protein systems, e.g., for the aggregation of bacteriorhodopsin in bilayers containing charged lipids (Watts et al., 1993). Nevertheless, the phenomenology of protein organization as controlled by the underlying lipid phase equilibria (cf. Figs. 4 and 6) is expected still to apply. In particular, the theoretical modeling presented accounts for various contributions to the system entropy, both the translational entropy, the entropy of mixing, and the internal entropy of the lipid chains. Hence this type of modeling may prove useful to investigate subtle but important mechanisms of entropy-driven protein crystallization effects proposed by Uitdehaag and Watts (unpublished).

From the point of view of membrane functions, the state of protein organization pictured in Figs. 4 f and 6 a might be of particular interest as it demonstrates under which conditions, controlled by the lipids, small aggregates of proteins may arise due to a sharing of special lipids that are available only in small amounts. The sensitivity of this state aggregation to the lipid composition, as expressed in our phenomenological analysis, may provide a basis for a trigger mechanism for membrane function (Sackmann, 1995).

As pointed out in this paper, the distinction between densely packed protein arrays and two-dimensional protein crystals is a question that is very difficult to investigate theoretically, and the regular arrays of proteins seen in the computer simulation snapshots in Figs. 4 and 6 may be artifacts of the underlying lattice. Moreover, to investigate the relative stability of the different types of two-dimensional crystalline symmetries that have been observed, e.g., for bacteriorhodopsin (Watts et al., 1993), it is required that directional protein-protein potentials are invoked. The system sizes that are feasible to study in the computer simulations are not big enough to encompass enough proteins to allow observation of the nonequilibrium process of grain-boundary formation and subsequent annealing of the protein array upon approach to the equilibrium state. But in principle, the microscopic model should permit such a study, which would be of interest in relation to comparing with experimental data.

APPENDIX

Two-dimensional fluid-solid-like transition within a large protein aggregate

In this Appendix we restrict ourselves to outline the key lines of a study of the formation of regular protein arrays (crystalline solids) within a large protein aggregate (see our discussion of the large aggregate regime in our phenomenological model above). The questions of whether two-dimensional systems exhibit a true fluid-solid phase transition and whether this transition is continuous or discontinuous, involving a hexatic intermediate phase or not, are, to different extents, still under debate (Bladon and Frenkel, 1995, and references within). It is nevertheless clear that a structure factor that is associated with a crystalline order can be measured in large but finite two-dimensional systems of colloids. In systems of two-dimensional colloids, the existence of gas-liquid and solid-dense solid transitions on top of the fluid-solid transition have been shown to depend on the range and strength of the pair interaction potentials one attaches to

them (Bladon and Frenkel, 1995). An intriguing question is what transitions exhibits a system that consists of hard disks that are aggregated due to capillary, nonadditive, forces or, in other words, in which way would it be possible, by changing the parameters of such systems, to relate the behavior to a specific class of pair interaction potentials. An attempt to answer this question can be made by calculating the potential of mean force, mainly following the work by Lekkerkerker et al. (1992).

Let us consider an aggregate consisting of N hard-disk colloids immersed in a β-phase and bounded by an α-β interface (Fig. 4, b-e). We assume that the internal energy of such an aggregate can be written as a sum of two Hamiltonians, $\mathcal{H}_c$ and $\mathcal{H}_w$, one describing the colloid-colloid interactions for the hard disks within the aggregate and the other one describing the colloid-wetting phase interactions between the wetting phase and the disks, respectively. In the cases where the colloid-wetting phase interactions can be described by an effective interface model, $\mathcal{H}_w$ depends on location of the N disks, inside the aggregate, $\mathbf{R}^N$, and the location of the α-β interface defining the aggregate, $\mathbf{L}$. The configurational partition function for the single aggregate system can thus be written as

$$\mathcal{Z} = \int \mathcal{D}\mathbf{R}^N \mathcal{D}\mathbf{L} e^{-[\mathcal{H}_c(\mathbf{R}^N) + \mathcal{H}_w(\mathbf{R}^N + \mathbf{L})]/k_B T}, \quad (24)$$

where $\mathcal{D}\mathbf{R}^N$ and $\mathcal{D}\mathbf{L}$ are the functional measures for the integration over all the possible realizations of $\mathbf{R}^N$ and $\mathbf{L}$, respectively.

As before (see the section on the phenomenological capillary potential above), we assume that the disks inside the aggregate lie close enough to each other (see Fig. 4, d and e) so that the fluctuations of the fluid-fluid interface are well described by considering an effective circular substrate of radius

$$R_N = \sqrt{\frac{N}{\pi\rho}}, \quad (25)$$

where ρ is the number density inside this effective substrate. This relaxes the dependence of $\mathbf{L}$ on $\mathbf{R}^N$ and enables us to rewrite Eq. 24 as

$$\mathcal{Z} = \int \mathcal{D}\mathbf{R}^N e^{-\mathcal{H}_c(\mathbf{R}^N)/k_B T} \int \mathcal{D}\mathbf{L} e^{-\mathcal{H}_w(\mathbf{L})/k_B T} \equiv e^{-[\Omega_c + \Omega_w]/k_B T}, \quad (26)$$

where Ω_c and Ω_w are the grand potentials (the ensemble is grand canonical with respect to the wetting phase) describing the hard disk system inside the effective substrate and the fluctuation of the fluid-fluid interface, respectively. The free energy is given in the usual way by

$$\Omega = -k_B T \ln \mathcal{Z} = \Omega_c + \Omega_w. \quad (27)$$

Hence we have separated our problem into two independent problems that are coupled only by depending on the same parameters. More specifically, Ω now consists of two additive parts, one, Ω_c, which considers only a system of hard disks in a given area, $A_A \equiv \pi R_N^2$, and at given density ρ, and the other one, Ω_w, which describes the wetting of a circular substrate of radius R_N. The latter, Ω_w, is given by Eq. 3. The former, Ω_c, can be calculated from the hard disk compressibility factor, $Z \equiv P/(\rho k_B T)$, of Eq. 19 by

$$\Omega_c = \eta \frac{k_B T}{2\pi r_0^2} A_A \int \frac{Z}{\eta} d\eta, \quad (28)$$

where $\eta \equiv \pi r_0^2 \rho$ is the volume fraction of the disks inside the effective substrate. Z can be given by the virial expansion in Eq. 19. However, finding a proper analytic approximation of Z to be used in Eq. 28 close to the two-dimensional melting point is not a trivial matter and requires further study.

Given two different forms of Ω_c to describe a fluid and a crystalline order of the disks inside the effective substrate, one can identify the

location of the fluid-solid transition for the hard disk colloids by demanding

$$\mu_{\text{solid}} = \mu_{\text{fluid}}, \quad \text{and} \quad P_{\text{solid}} = P_{\text{fluid}}, \quad (29)$$

according to the definitions of $\mu = \partial\Omega/\partial N$ and $P = -\partial\Omega/\partial A_{\text{A}}$.

REFERENCES

Alder, B. J., and T. E. Wainwright. 1962. Phase transitions in elastic disks. *Phys. Rev.* 127:359–361.

Aranda-Espinoza, H., A. Berman, N. Dan, P. Pincus, and S. Safran. 1996. Interaction between inclusions embedded in membranes. *Biophys. J.* 71:648–656.

Beysens, D., and D. Esteve. 1985. Adsorption phenomena at the surface of silica spheres in a binary liquid mixture. *Phys. Rev. Lett.* 54:2123–2129.

Bladon, P., and D. Frenkel. 1995. Dislocation unbinding in dense two-dimensional crystals. *Phys. Lett.* 74:2519–2522.

Bruinsma, R., M. Goulian, and P. Pincus. 1994. Self-assembly of membrane junctions. *Biophys. J.* 67:746–750.

Dammann, B., H. C. Fogedby, J. H. Ipsen, C. Jeppesen, K. Jørgensen, O. G. Mouritsen, J. Risbo, M. C. Sabra, M. M. Sperotto, and M. J. Zuckermann. 1996. Computer simulation of thermodynamic and conformational properties of liposomes. *In* Nonmedical Applications of Liposomes. Y. Barenholz and D. Lasic, editors. CRC Press, Boca Raton, FL. 85–128.

Damodaran, K. V., and K. M. Merz, Jr. 1994. Computer simulation of lipid systems. *In* Reviews of Computational Chemistry, Vol. V. K. B. Lipkowitz and D. B. Boyd, editors. VCH Publishers, New York. 269–298.

Dietrich, S. 1988. Wetting phenomena. *In* Phase Transition and Critical Phenomena, Vol. 12. D. Domb and J. Lebowitz, editors. Academic Press, New York, 1–218.

Fattal, D. R., and A. Ben-Shaul. 1993. A molecular model for lipid-protein interactions in membranes: the role of hydrophobic mismatch. *Biophys. J.* 65:1795–1809.

Gennis, R. B. 1989. Biomembranes. Molecular structure and Function. Springer-Verlag, Heidelberg. 533 pp.

Gil, T., and J. H. Ipsen. 1997. Capillary condensation between disks in two dimensions. *Phys. Rev. E.* 55:1713–1721.

Gil, T., and L. Mikheev. 1995. Curvature controlled wetting in two dimensions. *Phys. Rev. E.* 52:772–780.

Golestanian, R., M. Goulian, and M. Kardar. 1996. Fluctuation-induced interactions between rods on membranes and interfaces. *Europhys. Lett.* 33:241–245.

Hoover, W. G., and F. H. Ree. 1968. Melting transition and communal entropy for hard spheres. *J. Chem. Phys.* 49:3609–3617.

Jackson, M. B. (ed.). 1993. Thermodynamics of Receptors and Channels. CRC Press, Boca Raton, FL. 439 pp.

Jørgensen, K., and O. G. Mouritsen. 1995. Phase separation dynamics and lateral organization of two-component lipid membranes. *Biophys. J.* 95:942–954.

Jørgensen, K., M. M. Sperotto, O. G. Mouritsen, J. H. Ipsen, and M. J. Zuckermann. 1993. Phase equilibria and local structure in binary lipid bilayers. *Biochim. Biophys. Acta.* 1152:135–145.

Kinnunen, P. J. K., and O. G. Mouritsen (eds.). 1994. Functional Dynamics of Lipids in Biomembranes. Topical issue of *Chem. Phys. Lipids.* 73:1–236.

Kühlbrandt, W. 1992. Two-dimensional crystallization of membrane proteins. *Quart. Rev. Biophys.* 25:1–49.

Lekkerkerker, H. N. W., W.-C. Poon, P. N. Pusey, A. Stroobants, and P. B. Warein. 1992. Phase behavior of colloid + polymer mixtures. *Europhys. Lett.* 20:559–564.

Lipowsky, R., and M. E. Fisher. 1987. Scaling regimes and functional renormalization for wetting transitions. *Phys. Rev. B Solid State.* 36:2126–2141.

Mouritsen, O. G. 1990. Computer simulation of cooperative phenomena in lipid membranes. *In* Molecular Description of Biological Membrane Components by Computer Aided Conformational Analysis. R. Brasseur, editor. CRC Press, Boca Raton, FL. 3–83.

Mouritsen, O. G., and M. Bloom. 1984. Mattress model of lipid-protein interactions in membranes. *Biophys. J.* 46:141–153.

Mouritsen, O. G., and M. Bloom. 1993. Models of lipid-protein interactions in membranes. *Annu. Rev. Biophys. Biomol. Struct.* 22:145–171.

Mouritsen, O. G., and K. Jørgensen. 1994. Dynamical order and disorder in lipid bilayers. *Chem. Phys. Lipids* 73:3–25.

Mouritsen, O. G., and M. M. Sperotto. 1992. Thermodynamics of lipid-protein interactions in lipid membranes: the hydrophobic matching condition. *In* Thermodynamics of Cell Surface Receptors. M. Jackson, editor. CRC Press, Boca Raton, FL. 127–181.

Mouritsen, O. G., M. M. Sperotto, J. Risbo, Z. Zhang, and M. J. Zuckermann. 1996. Computational approach to lipid-protein interactions in membranes. *Adv. Comp. Biol.* 2:15–64.

Nielsen, M., L. Miao, J. H. Ipsen, O. G. Mouritsen, and M. J. Zuckermann. 1996. Random-lattice models and simulation algorithms for the phase equilibria in two-dimensional condensed systems of particles with coupled internal and translational degrees of freedom. *Phys. Rev. E.* 54:6889–6905.

Pink, D. A., T. J. Green, and D. Chapman. 1980. Raman scattering in bilayers of saturated phosphatidylcholines: experiment and theory. *Biochemistry.* 19:349–356.

Risbo, J., M. M. Sperotto, and O. G. Mouritsen. 1995. Theory of phase equilibria and critical mixing points in binary lipid bilayers. *J. Chem. Phys.* 103:3643–3656.

Sackmann, E. 1994. Membrane bending energy concept of vesicle- and cell-shapes and shape transitions. *FEBS Lett.* 346:3–16.

Sackmann, E. 1995. Biological membranes architecture and function. *In* Structure and Dynamics of Membranes, From Cells to Vesicles. R. Lipowsky and E. Sackmann, editors. North Holland, Amsterdam. 1–63.

Schick, M. 1990. Introduction to wetting phenomena. *In* Lipids at Interfaces. J. Charvolin, J. F. Joanny, and J. Zinn-Justin, editors. North Holland, Amsterdam. 415–497.

Watts, A. (ed.). 1993. Protein-Lipid Interactions. Elsevier, Amsterdam. 379 pp.

Watts, A., C. Venien-Bryan, M. Sami, C. Whiteway, J. Boulter, and B. Sternberg. 1993. Lipid-protein interactions in controlled membrane protein array and crystal formation. *In* Protein-Lipid Interactions. A. Watts, editor. Elsevier, Amsterdam. 351–370.